Available online at www.sciencedirect.com
SCIENCE DIRECT®
European Journal of Operational Research 154 (2004) 641–658
EUROPEAN JOURNAL OF OPERATIONAL RESEARCH
www.elsevier.com/locate/dsw

O.R. Applications

A nonlinear optimization package for long-term hydrothermal coordination ☆

Jordi Castro *, José A. González

Statistics and Operations Research Department, Universitat Politècnica de Catalunya, Pau Gargallo 5, 08028 Barcelona, Spain

Received 6 April 2001; accepted 4 July 2002

Abstract

Long-term hydrothermal coordination is one of the main problems to be solved by an electric utility. Its solution provides the optimal allocation of hydraulic, thermal and nuclear resources at the different intervals of the planning horizon. The purpose of the paper is two-fold. Firstly, it presents a new package for solving the hydrothermal coordination problem. The model implemented accurately describes both the hydraulic and thermal subsystems. The resulting large-scale nonlinear and nonconvex problem is solved through either Minos or Snopt, two state-of-the-art nonlinear optimization packages. The second objective of the paper is to deliver to the optimization community the package. Since it implements a difficult, real, and large-scale problem, it can be considered a good test for new nonlinear optimization solvers. Computational results of the package in the solution of a set of real instances of up to 32,000 nonlinear variables, 13,000 linear and 2500 nonlinear constraints are reported.

Keywords: Large scale optimization; Nonlinear programming; Electricity generation; Long-term hydrothermal coordination

1. Introduction

The purpose of a long-term hydrothermal coordination model is to minimize the cost of fuels purchased by a power utility over a long time period (e.g., one or two years), considering both the hydraulic and thermal subsystems of the company. For each interval of the planning horizon the model has to optimize:

- The expected requirements for each possible type of fuel.
- The amount of fuel used for generation and stored until the next interval for each thermal unit.
- The volumes of water stored and discharged for generation at each reservoir (in terms of water inflow availability).

The package presented in this paper, denoted as HTCOOR (from HydroThermal COORdination package), includes additional features to the above list. Among these we find:

- It deals with stochastic water inflows for each reservoir.

☆ This work was partially supported by the European ESPRIT Project 22652 and by the CICYT Project TAP99-1075-C02-02.

* Corresponding author.
E-mail addresses: jcastro@eio.upc.es (J. Castro), jose.a.gonzalez@upc.es (J.A. González).

0377-2217/$ - see front matter
doi:10.1016/S0377-2217(02)00802-0

- Outage rates of the generation units are considered.
- The amount of emergency energy (i.e., energy purchased to an external utility to satisfy the uncovered load due to outages) is also optimized.
- Both the hydraulic and thermal subsystems are optimized jointly through a detailed model.
- The different functions of the model (e.g., covering of the load demand as a function of the energy generated, hydraulic generation as a function of the water discharges, etc.) are formulated as nonlinear functions, rather than just linear approximations.

HTCOOR was developed in the scope of a three-year (1996–1999) ESPRIT project funded by the European Union. This project involved several academic and private institutions from Germany, Austria and Spain, and was aimed at developing various optimization tools for electricity generation planning. HTCOOR was designed for those utilities in which the hydraulic system represents a significant percentage of the overall generation. Spanish power utilities usually belong to this class.

HTCOOR assumes that each utility knows or has a forecast of its load demand, as was the case in Spain by 1996. However, by 1998 this situation changed due to a deregulation of the Spanish electric market, following directives from the European Union. The new environment is based on an auction system where utilities offer generation at a certain price to a central agent. Depending on the prices of the rest of the companies, this generation will be accepted or rejected. It is thus difficult for a company to know in advance its final load demand. Although, in a strict sense, HTCOOR would not be appropriate for the new market, it can still be a valuable tool for two reasons. First, it could be extended to deal with an auction system; although this has not yet been fully implemented, a preliminary method is presented in this work. And second, despite a deregulated system, monopolistic or dominant utilities can have a good forecast of their demand. This is the current situation in Spain, where two companies share 85% of the market, and there were plans for them to merge.

The model implemented in HTCOOR is an extension of an earlier one described in [23] (which is itself an extension of that given in [22] for hydraulic systems). From a modeling point of view, among the main new features we find the inclusion of contracts with external utilities in the thermal subsystem, and of pumping arcs (to transfer water from down to upstream reservoirs) in the hydraulic one. From the development side, in [23] only a preliminary implementation was obtained, whereas HTCOOR is a full package, linked to two of the best available solvers for nonlinear optimization: Minos 5.5 [19] and Snopt 5.3 [11].

Several alternative models have been suggested in the past for the hydrothermal coordination problem. Most of them, however, neither consider a detailed description of the hydraulic or thermal systems, nor exactly formulate the real constraints of the problem. For instance, in [25] the demand is linearly approximated, while in [18] no hydraulic subsystem is considered. In [1] the control of a hydroelectric single-interval and multireservoir system is addressed, without considering the thermal network. In [8,9] a long-term hydraulic generation system is solved using multistage stochastic programming techniques (i.e., scenario analysis) and parallel computing. The model considers a nonlinear problem with only linear constraints, and it lacks an accurate description of the thermal park. Similarly, the approach adopted in [17] formulates the hydrothermal coordination problem as a nonlinear network optimization with linear side constraints. Unlike the above approaches, HTCOOR considers a problem with nonlinear objective and nonlinear constraints, which needs to be solved through general state-of-the-art nonlinear programming solvers.

None of the alternative models and implementations described in the above paragraph are currently available for research purposes. This makes them difficult for the optimization community to test when developing new solvers. To avoid this shortcoming we are freely distributing HTCOOR for research purposes, together with some slightly modified real case instances. Currently the package can only work with Minos and Snopt, but minor modifications should enable it to be used with alternative solvers. The difficult large-scale

nonlinear and nonconvex optimization problems arising from this model can constitute a good test for newly developed optimization software. HTCOOR can be freely obtained for academic purposes from http://www-eio.upc.es/~jcastro/htcoor.html.

The structure of the document is as follows. Section 2 describes the model implemented in HTCOOR. Several subsections are devoted to the different components of the model—hydraulic and thermal subsystems, treatment of stochasticity, extensions considered, formulation of the resulting optimization problem, etc. Section 3 outlines the main structure of the package. Section 4 presents computational results obtained with the package in the solution of a set of real problems.

2. The hydrothermal model implemented in HTCOOR

We will consider a long-term hydrothermal problem with a planning horizon of one to two years, divided into a set of (usually monthly) Ni intervals. We will also assume the company owns Nr reservoirs and Nu thermal units that can work with Nf different fuel types (e.g., gas, nuclear, coal, etc.). These parameters, together with K—the number of blocks used to represent water flow stochasticity, as described below—mainly determine the size of a particular problem instance.

Briefly, the hydro system will be modeled through a network whose nodes represent reservoirs at different intervals of the period. The arcs of the network—the variables to be optimized—are related to the discharge and pumping units, spillage channels and volumes at the end of each interval. The thermal system will also be modeled as a multiinterval network. The different fuels flowing through the network from one interval to the next for the same thermal unit are considered as different commodities.

For the rest of the document, superscript i refers to the ith interval; subscript j refers to a thermal unit (or some object related to a thermal unit); superscript k denotes a hydraulic block; and finally, subscripts n and a are related to reservoirs and arcs respectively, while subscript f means fuel.

2.1. Stochasticity

Long-term problems are difficult to solve due to the need to deal with the uncertainties present in the real hydrothermal system. Several conditions are undetermined, but water inflow stochasticity is the most important for systems in which the hydraulic generation represents a significant percentage of the total.

Stochastic programming techniques (e.g., scenario analysis) have frequently been applied to deal with water inflow uncertainties (e.g., [8,9,24]). We considered a different approach, assuming that all the variables related with the basin are random variables, since they depend on the random variables that describe the inflows. The variability of the inflows is thus directly transmitted to the releases, spillages and storages of the reservoirs. This method, originally introduced in [22], was shown to be appropriate for the hydrothermal coordination problem (see [14] for a comprehensive description).

This approach considers that both the inflows and all the hydraulic variables can be modeled as K-multiblock random variables, K being the number of values defining $K-1$ blocks—see Fig. 1(a) for an example considering $K=4$. The higher K the better the multiblock approximation of the real random variable. It was observed in [14] that, given a set of probabilities for each block, K values allow to conveniently define the shape of real-valued random variables of hydrothermal coordination models, like the amount of water that will be turbinated in some interval. Then each variable of the hydrosystem is actually a set of K real variables associated with each block of the multiblock random variable. These variables are replicated for all the Ni intervals of the planning horizon. Although the hydrogeneration is a nonlinear function of the volumes and discharges at the reservoirs, it can also be accurately represented by a K-multiblock distribution (see [14] for details). As shown later, an expected hydrogeneration can be computed from the K hydrogeneration values for each interval. This expected hydrogeneration, together with the deterministic thermal one, is used to satisfy the interval load demand.

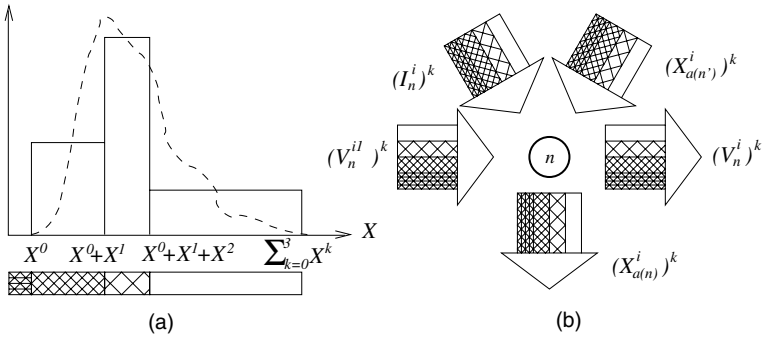

Fig. 1. (a) Multiblock random variable approximation. (b) Volumes, discharges and inflow multicommodity arcs related to reservoir n at interval i. The darkest regions are associated with X^0; the next shade, with X^1; and so on, until the lightest regions, related to X^{K-1}.

Under our model, we do not seek optimal values of the variables that describe the basin over the planning horizon. We try to determine a policy for the management of these variables. The optimal policy to be found results in a probability distribution for each variable in the time-replicated hydronetwork, such that the savings of expensive energy are maximized. Our model assumes that inflows, releases of water and water stored in the reservoirs are highly dependent for a particular time interval, and this information can be used to compute an accurate estimate of the expected hydrogeneration.

The multiblock approach has some significant differences with the scenario analysis. For a single interval problem, each block can be viewed as a particular scenario. In this case, the main difference between both methods is that, in the multiblock approach, the cost of a particular policy is obtained from the deterministic thermal generation and the expected hydrogeneration. Instead, in the scenario method an expected cost would be obtained in the recourse function from the particular costs of each scenario (computed from the first stage thermal generation, and the particular second stage hydrogeneration). In addition, in a multiinterval problem, the multiblock approach considerably reduces the size of the resulting nonlinear optimization problem. In this case, the scenario method would generate a tree of situations, and the size of the problem would increase exponentially. However, it would remain proportional to K in the multiblock technique. For instance, if the horizon planning has been divided into n intervals and our decision variables can have at most m choices per interval, the number of possible scenarios is m^n, whereas the number of variables with the multiblock model is proportional to Kn. That allows to keep a detailed—i.e., nonlinear—formulation of the hydrogeneration and demand satisfaction functions, avoiding the linear and inexact approximations that are required when a large number of scenarios is considered. The solution of hydrothermal coordination problems using detailed nonlinear functions through the method of scenarios can be considered computationally prohibitive.

It is noteworthy that the multiblock approach, as far as we know, it has only been successfully applied to hydrothermal coordination problems, whereas the scenario analysis is a much more versatile tool. Moreover, the tree of scenarios considered by the latter exhausts all the possible future situations. The implicit range of choices covered by the multiblock method is smaller. However, the omitted choices are expected not to have a significant effect on the final computation of the hydrogeneration. The extensive set of simulations performed in [15] with the solutions obtained with the multiblock approach showed that it provides satisfactory results in real hydrothermal coordination problems.

2.2. The hydraulic subsystem

The hydrogeneration is computed from the known characteristics of a replicated—for each interval—hydro network model. The variables in

this model are the flows of water from one reservoir to another, and the stored volumes at each reservoir at the end of each interval. Moreover, as stated above, each variable is in fact a set of K commodities (the real variables of the optimization problem). The hydro variables are:

- $(X^i)_a^k$, $k = 0, \ldots, K-1$: kth commodity of flow at some arc a (a release, a spillage or a pumping) during the ith interval.
- $(V^i)_n^k$, $k = 0, \ldots, K-1$: kth commodity of stored water in reservoir n at the end of the ith interval.

The following set of known parameters are also required:

- $(I^i)_n^k$, $k = 0, \ldots, K-1$: natural inflows.
- $(V^0)_n^k$, $k = 0, \ldots, K-1$: initial volumes; usually zero for $k > 0$.
- $(V^{\mathrm{Ni}})_n^k$, $k = 0, \ldots, K-1$: final volumes; usually zero for $k > 0$.

Fig. 1(b) shows the structure of the hydro network for a particular reservoir n (with upstream reservoir n') and interval i. Several types of objects travel through the network independently, that is, their flows never merge. However, they are related by the arc capacity: the sum of flows for all the commodities cannot exceed this capacity. Each commodity is related to some level of probability. X^0 means guaranteed flow; X^1 is an extra flow likely to be found but not guaranteed; and so on. In general, the higher the superscript, the lower the flow probability.

Defining by $\mathscr{T}_n$ and $\mathscr{S}_n$ the set of release, spillage and pumping arcs that respectively finish and start at reservoir n, the balance equations of the hydrothermal network can thus be expressed as

$$\sum_{a\in\mathscr{T}_n} (X_a^i)^k + (V_n^{i-1})^k + (I_n^i)^k = \sum_{a\in\mathscr{S}_n} (X_a^i)^k + (V_n^i)^k \quad \begin{cases} k = 0, \ldots, K-1 \\ i = 1, \ldots, \mathrm{Ni} \\ n = 1, \ldots, \mathrm{Nr}, \end{cases} \tag{1}$$

with bounds on each variable and mutual capacity constraints for each arc

$$\begin{aligned} &(\underline{V}^i)_n^k \leqslant (V_n^i)^k \leqslant (\overline{V}^i)_n^k \quad (i = 1, \ldots, \mathrm{Ni}-1) \\ &(\underline{X}^i)_a^k \leqslant (X_a^i)^k \leqslant (\overline{X}^i)_a^k \quad (i = 1, \ldots, \mathrm{Ni}) \\ &\begin{cases} k = 0, \ldots, K-1 \\ n = 1, \ldots, \mathrm{Nr} \\ a \in \mathscr{T}_n \vee a \in \mathscr{S}_n, \end{cases} \end{aligned} \tag{2}$$

$$\begin{aligned} &\sum_{k=0}^{K-1} (V_n^i)^k \leqslant \overline{V}_n^i \quad (i = 1, \ldots, \mathrm{Ni}-1) \\ &\sum_{k=0}^{K-1} (X_a^i)^k \leqslant \overline{X}_a^i \quad (i = 1, \ldots, \mathrm{Ni}) \\ &\begin{cases} n = 1, \ldots, \mathrm{Nr} \\ a \in \mathscr{T}_n \vee a \in \mathscr{S}_n, \end{cases} \end{aligned} \tag{3}$$

where overlined (underlined) symbols are used to represent an upper (lower) bound.

Hydro generation is assumed to be a multiblock random variable, as are water releases and storages in the reservoirs. In fact, generation is a nonlinear function of these variables, and its real distribution does not belong to the multiblock family. However, we found that the multiblock approximation fits the real hydrogeneration distribution well enough [14]. For each commodity (block) and interval, the hydrogeneration $(G^i)^k$ can be computed as a nonlinear function of the kth block discharges and initial and final volumes at reservoirs during this interval:

$$(G^i)^k = \Gamma^i\left((X^i)^k, (V^{i-1})^k, (V^i)^k\right) \quad k = 0, \ldots, K-1, \ \ i = 1, \ldots, \mathrm{Ni}. \tag{4}$$

A detailed expression of the above $\Gamma(\cdot)$ function can be found in [16]. Hydrothermal models involving only the above description of the hydraulic subsystem (e.g., [22]) can be formulated as a nonlinear multicommodity network flow problem, and solved through specialized software [5]. Including the elements of the following sections forces us to use a general solver for nonlinear optimization.

2.3. The thermal subsystem

The generation process and fuel management can also be viewed as a multicommodity network expanded over the planning horizon. A multicommodity model is used because some units can operate with several fuels. However, there are important differences between the hydro and the thermal networks, since fuels do not flow from one unit to another, but from one interval to the next for a particular unit. The meaning of the variables related to these arcs is "remaining fuel". Another class of variables represents the supply of fuel to the units. Finally, for each unit and each interval, there is one arc related to the energy generation. This model for the thermal system is fairly versatile and it could be adapted to represent other complex situations arising in the market.

Fig. 2 shows an example of a thermal network with Nu units, Ni intervals and two fuels. A delivery of fuel f to the unit j at the ith interval is denoted as $Z^i_{f,j}$. $F^i_{f,j}$ is the fuel f not consumed by the unit j at the interval i. Finally, $E^i_{f,j}$ represents the generation obtained by the unit j at the interval i using the fuel f. Looking at Fig. 2 we see that fuel 1 can be delivered during all the intervals, even at the end of the last one (arrow to the sink node); this situation could represent a "take-or-pay" contract. On the other hand, fuel 2 is a specific delivery expected at the beginning of the second interval (for instance, the purchase of a tanker).

The balance equation for the thermal network can be stated as

$$F^{i-1}_{f,j} + Z^i_{f,j} = F^i_{f,j} + \varepsilon_{f,j} E^i_{f,j} \quad \begin{cases} i = 1,\ldots,\mathrm{Ni} \\ j = 1,\ldots,\mathrm{Nu} \\ f = 1,\ldots,\mathrm{Nf}, \end{cases} \tag{5}$$

$\varepsilon_{f,j}$ being a parameter for the efficiency of unit j with respect to the fuel used. Bounds on the generation and the fuel usage can also be considered. For instance, for the fuel usage we have

$$\sum_{f=1}^{\mathrm{Nf}} F^i_{f,j} \leqslant \overline{F}_j, \quad \begin{cases} i = 1,\ldots,\mathrm{Ni} \\ j = 1,\ldots,\mathrm{Nu}. \end{cases} \tag{6}$$

Maintenance schedules of unit j at interval i can be modeled by setting $E^i_{f,j} = 0$ for all fuel f. Environmental considerations could be included through simple linear constraints similar to

$$\sum_{f\in CF} \sum_{i\in CI} \sum_{j\in CU} \delta^i_{f,j} E^i_{f,j} \leqslant \overline{CONT},$$

where $\overline{CONT}$ is some limit to the emission of pollutants, $\delta^i_{f,j}$ is a generation to pollutant transformation parameter, and CF, CI and CU denote some subsets of the fuel, interval and thermal units sets respectively.

2.4. Modeling the power supply and demand

Power utilities usually know the load demand at each interval by means of the so called load duration curve (LDC) (see Fig. 3(a)). The LDC gives the amount of time (horizontal axis) the utility must be generating at a certain power level (vertical axis). The area $\widehat{E}^i$ under the curve and $\widehat{P}^i$ are

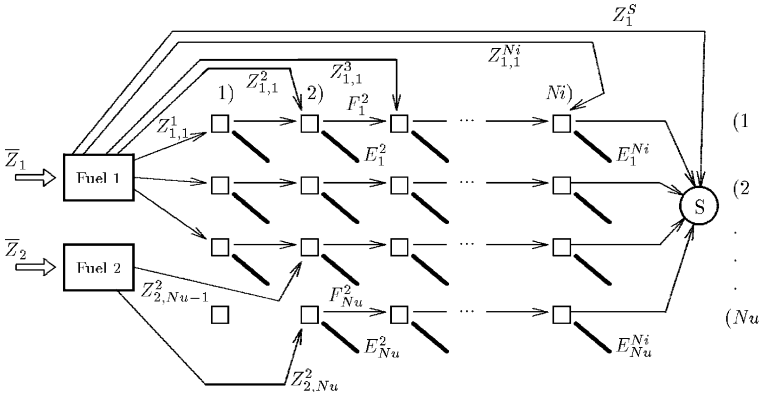

Fig. 2. Example of a replicated thermal network. Several fuels and multiple purchases were included.

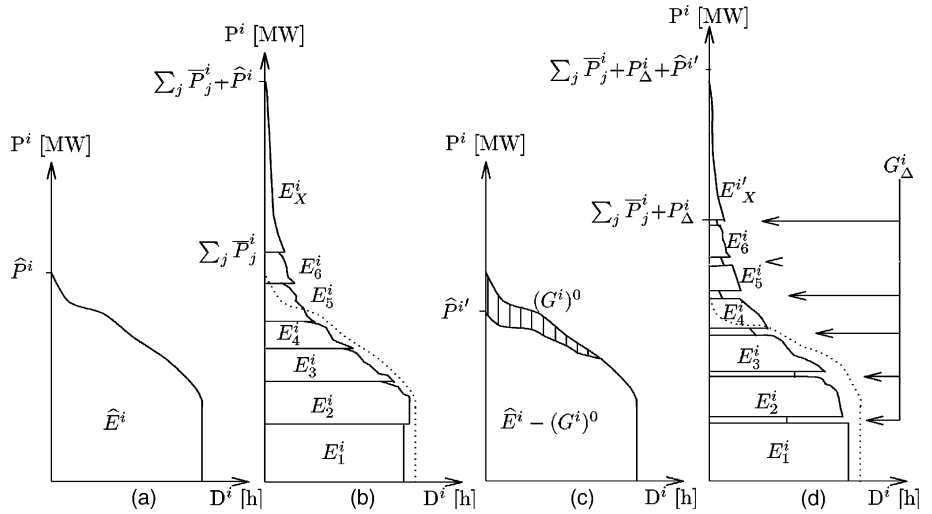

Fig. 3. Transforming the LDC. (a) Original LDC. (b) GDC (dotted, the LDC). (c) LDC peak-shaved with deterministic hydrogeneration $(G^i)^0$. (d) GDC, corresponding to peak-shaved LDC, including stochastic hydrogeneration G^i_Δ.

respectively the total energy and the peak load to be provided by the utility during a particular interval i of the planning horizon. The area $\widehat{E}^i$ must be covered through the units of the utilities, ordered by some merit criteria as efficiency.

The LDC models demand from the users' point of view. The utility point of view, however, has to account for power unavailability of the units due to outages. This is done through the generation duration curve (GDC) of Fig. 3(b). The GDC is obtained from the LDC through a standard convolution process in the electrical planning field (see [2,26] for details). The convolution procedure is iteratively applied for each thermal unit, using its capacity and failure probability. The GDC can be seen as divided into many sections, each representing the mean contribution some unit is expected to have (denoted by E^i_j for the jth unit). We must guarantee

$$\widehat{E}^i = \sum_{j=1}^{\mathrm{Nu}} E^i_j + E^i_X \quad i = 1, \ldots, \mathrm{Ni},$$

where E^i_X denotes the emergency energy, which should be imported at interval i in the case of fortuitous loss of load. The upper point in the power axis for the GDC is $\sum_{j=1}^{\mathrm{Nu}} \overline{P}^i_j + \widehat{P}^i$, where $\overline{P}^i_j$ is the capacity of unit j at interval i (usually constant for all the intervals). The coverage of the GDC must be done through the thermal units and the emergency energy—the latter usually at a high cost. Emergency energy is necessary because of the risk of several units being unavailable at the same time, due to their individual outage probabilities.

Free-cost hydrogeneration is useful to reduce both E^i_X and the production of some thermal units. The hydraulic contribution is determined taking into account its stochastic nature. We have divided this contribution into two parts: the guaranteed generation, noted as $(G^i)^0$, and the undeterministic generation G^i_Δ. Fig. 4 shows the density function f^i_G of the generation random variable G^i for a particular interval, the deterministic $(G^i)^0$ and undeterministic G^i_Δ values, and the relation $E[G^i] = (G^i)^0 + G^i_\Delta$. $(G^i)^0$ is equal to the value computed in (4) for $k = 0$. G^i_Δ is computed as

$$G^i_\Delta = E[G^i] - (G^i)^0. \tag{7}$$

The expected generation $E[G^i]$ is computed through the $\Gamma(\cdot)$ function of (4), using the multiblock representation of the random variable G^i. A detailed expression for $E[G^i]$ can be found in [16].

$(G^i)^0$ is used to peakshave the LDC (Fig. 3(c)), thus reducing the peak load to a new $\widehat{P}^{i'}$ value. The peak-shaving cannot exceed $\overline{P}^i_h$, the available capacity of the hydro system (usually constant for all

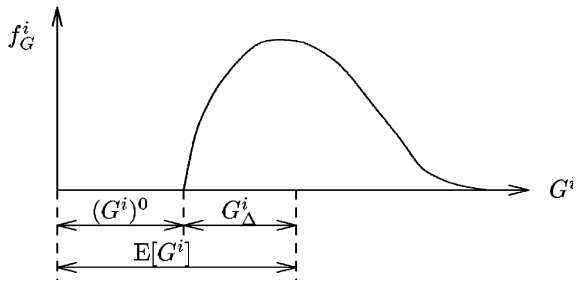

Fig. 4. Density function of the generation, guaranteed generation and undeterministic generation.

the intervals). The new energy demand is $\widehat{E}^i - (G^i)^0$. A new GDC (Fig. 3(d)) can now be obtained through the convolution procedure, using as a basis the peak-shaved LDC. As Fig. 3(d) shows, the stochastic hydrogeneration can be potentially located between any two consecutive units according to an economical merit order, since its right place is not known in advance. Each slice of stochastic generation can thus be considered as a pseudo-unit with an energy production (area of the slices) of $G^i_{\Delta j}$ and power capacity (height of the slices) of $P^i_{\Delta j}$, for $j = 1, \ldots, \mathrm{Nu}$. The optimal values of $G^i_{\Delta j}$ and $P^i_{\Delta j}$ for each pseudo-unit will be given by the solution of the hydrothermal coordination problem, taking into account the exact coverage of the GDC. Clearly, we must impose at each interval of the planning horizon

$$G^i_\Delta = \sum_{j=1}^{\mathrm{Nu}} G^i_{\Delta j} \quad i = 1, \ldots, \mathrm{Ni}, \tag{8}$$

where G^i_Δ is computed through (7). Moreover, the joint power capacity of the Nu pseudo-units plus the deterministic hydrogeneration should not exceed the maximum hydraulic capacity $\overline{P}^i_h$:

$$\sum_{j=1}^{\mathrm{Nu}} P^i_{\Delta j} + \frac{(G^i)^0}{T^i} = P^i_\Delta + \frac{(G^i)^0}{T^i} \leqslant \overline{P}^i_h \quad i = 1, \ldots, \mathrm{Ni}, \tag{9}$$

where P^i_Δ denotes the total stochastic hydro capacity, and $(G^i)^0/T^i$ (the mean deterministic capacity, T^i being the length of interval i) is used to approximate the deterministic hydro capacity.

As shown in Fig. 3(d), slices associated with the stochastic pseudo-units are shorter. This is because stochastic pseudo-units have a larger unavailability than regular thermal ones. Due to these discontinuities of the GDC, we consider an equivalent curve with nicer properties, the smoothed generation duration curve (SGDC). Fig. 5 shows the relation between the GDC and the SGDC. The main features of the SGDC are

- The SGDC is a continuous curve.
- Due to the increase in the availability of the hydro pseudo-units a decrease of the power from P^i_Δ to $\widetilde{P}^i_\Delta$ is performed, which is not an unrealistic practice. Eq. (9) above should thus be rewritten as

$$\sum_{j=1}^{\mathrm{Nu}} \widetilde{P}^i_{\Delta j} + \frac{(G^i)^0}{T^i} = \widetilde{P}^i_\Delta + \frac{(G^i)^0}{T^i} \leqslant \overline{P}^i_h \quad i = 1, \ldots, \mathrm{Ni}. \tag{10}$$

- It is a straight line from power 0 to the base power $P^i_{\min}$. From this point to $\sum_{j=1}^{\mathrm{Nu}} \overline{P}^i_j + \widetilde{P}^i_\Delta$ is some continuous function.
- The SGDC is not defined above $\sum_{j=1}^{\mathrm{Nu}} \overline{P}^i_j + \widetilde{P}^i_\Delta$.
- The duration at power $\sum_{j=1}^{\mathrm{Nu}} \overline{P}^i_j + \widetilde{P}^i_\Delta$ is equal to T^i_X, the maximum duration with loss of load.
- The duration from power 0 to power $P^i_{\min}$ is T^i_G, an average working duration for the first units.

The emergency energy E^i_X and the maximum duration with loss of load T^i_X are two of the most influential parameters of the model, mainly due to the high cost of E^i_X. We saw that they can be accurately estimated through the following expressions:

$$E^i_X = \frac{a^i Y^2}{(G^i)^0 - b^i} + c^i, \tag{11}$$

$$T^i_X = \frac{d^i Y^2}{(G^i)^0 - e^i} + f^i. \tag{12}$$

$Y = \overline{P}^i_h - (G^i)^0/T^i - \widetilde{P}^i_\Delta + \sum_{j \in \mathscr{L}^i} (\overline{P}^i_j - P^i_j)$ gives the decrease of power with respect to the available hydro and thermal capacity. The set $\mathscr{L}^i$ is the set of units with possible fuel limitations and contracts at interval i (contracts will be introduced in Section 2.8). Indeed, contracts and limited units may not reach their maximum capacity. a^i, b^i, c^i,

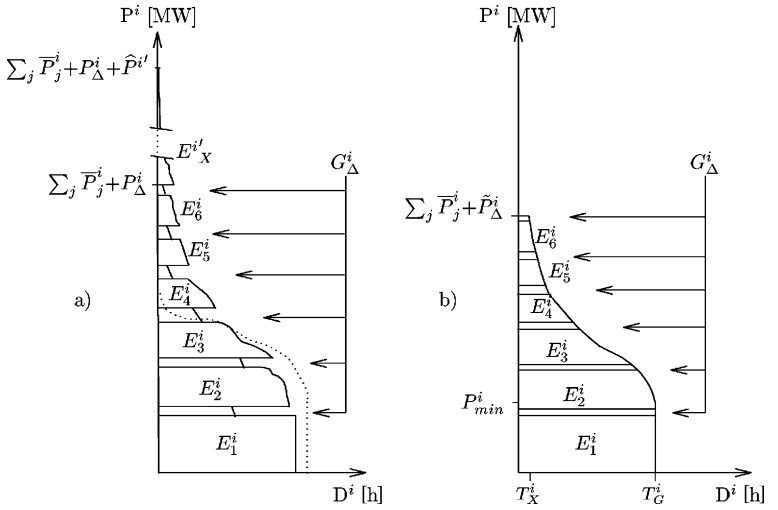

Fig. 5. Smoothing the GDC. (a) GDC with stochastic hydrogeneration G^i_Δ. (b) Smoothed curve (with hydro power reduced to $\widetilde{P}^i_\Delta$).

d^i, e^i, f^i are constants depending on each interval that have to be determined in advance for each particular problem. This is done through simulation and a further adjustment of the model given by (11) and (12) to the values obtained by simulating realistic operations. The solution for a^i, b^i, c^i, d^i, e^i, f^i is obtained by nonlinear least squares, using either Minos [19] or Snopt [11].

2.5. The power–energy curve

The power–energy curve (PEC) is the key function of the model, as it allows the computation of the power associated with a particular energy area under the SGDC. Let $M^i_{sg}(p)$ (see Fig. 6(a)) be a function representing the SGDC of interval i (p, power; $M^i_{sg}(\cdot)$, duration). Thus we can define the new function $\mathrm{PE}^i(e)$ as

$$\mathrm{PE}^i(e) = p, \text{ such that: } p \geqslant 0, \quad \int_0^p M^i_{sg}(u)\,\mathrm{d}u = e. \tag{13}$$

$\mathrm{PE}^i(e)$ is called the PEC. Fig. 6(b) illustrates a typical PEC. The main features of this curve are:

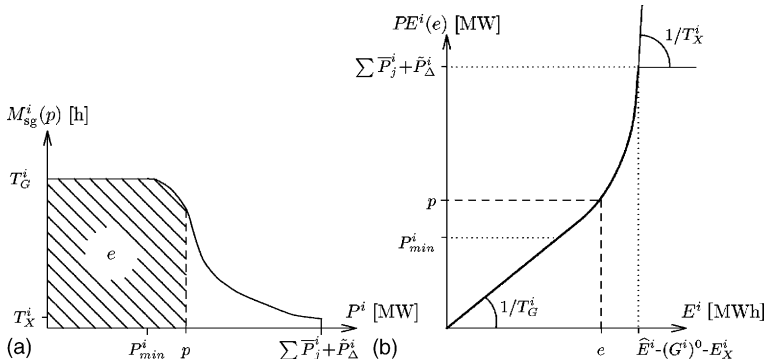

Fig. 6. Power–energy curve. (a) SGDC; (b) PEC.

- The derivative of $\mathrm{PE}^i(\cdot)$ is

$$\frac{\mathrm{dPE}^i(e)}{\mathrm{d}e} = \frac{1}{M^i_{\mathrm{sg}}(\mathrm{PE}^i(e))}.$$

If we denote by $\mathrm{EP}^i(p)$ the inverse function of $\mathrm{PE}^i(e)$, we can equivalently write

$$\frac{\mathrm{dEP}^i(p)}{\mathrm{d}p} = M^i_{\mathrm{sg}}(p).$$

- $\mathrm{PE}^i(\cdot)$ and $\mathrm{EP}^i(\cdot)$ are continuous and strictly increasing functions; their derivatives are also continuous.
- Since the SGDC is a non-increasing function, its integral is a concave function. The $\mathrm{PE}^i(\cdot)$—the inverse of this integral—will thus be convex, that is, its slope never decreases.
- The PEC is a straight line from (0,0) to $(T^i_G, T^i_G P^i_{\min})$. This segment can be written as:

$$\mathrm{PE}^i(e) = e/T^i_G, \quad 0 \leqslant e \leqslant T^i_G P^i_{\min}.$$

- The rightmost point of the PEC is located at

$$\left(\widehat{E}^i - (G^i)^0 - E^i_X, \sum_{j=1}^{\mathrm{Nu}} \overline{P}^i_j + \widetilde{P}^i_\Delta\right).$$

At this point the PEC has a slope equal to $1/T^i_X$.

Looking at Fig. 6 (b), it is clear that the PEC is best modeled through a two-piecewise function: a linear equation from $(0,0)$ to $(T^i_G, T^i_G P^i_{\min})$ and a curve from this last point to the rightmost one. (Attempts to fit a single high-order polynomial did not succeed.) Continuity at the contact point should be guaranteed at least until first derivatives to avoid problems when optimizing the model. The slope at the last point of the curve should also be fixed to $1/T^i_X$. In addition, the PEC of each interval depends on several parameters, such as $(G^i)^0$ and G^i_Δ, which are variables or expressions to be optimized when solving the coordination hydrothermal problem, and we must guarantee continuity until first derivatives for each possible value of these parameters. All these constraints led us to consider a four-point Bézier curve [3,4].

Indeed, the shape of the second part of the PEC can be accurately controlled by the position of the four Bézier points in the energy × power space. If we denote them by $b^i_0, , \ldots, , b^i_3$, and the parametric Bézier curve by $x^i(t) = (x^i_e(t), x^i_p(t)), t \in [0,1]$, then we can compute the power p associated with an energy value e of the second part of the PEC as

$$p = x^i_p((x^i_e)^{-1}(e)),$$

where $(x^i_e)^{-1}(e)$ denotes the inverse function of $x^i_e(t)$ (i.e., for a given energy e it returns the associated value $t \in [0,1]$ of the Bézier curve). The main benefit of using a Bézier curve is that we can easily fix the slope at $t = 0$ (contact point) and $t = 1$ (last point) at some specific values. Indeed, Bézier curves guarantee that the slope at $t = 0$ is given by the segment $b^i_1 - b^i_0$, whereas it is equal to $b^i_3 - b^i_2$ for $t = 1$. By simply moving b^i_1 and b^i_2 along these lines we can fit a particular PEC imposing derivatives at the contact and extreme points. This can be shown in Fig. 7, where two particular and very different SGDC—with the same energy area—are modeled through two Bézier points that share points b^i_0 and b^i_3.

The main drawback of using a parametric curve for the PEC is that we have to compute $(x^i_e)^{-1}(e)$. However, for a four-point Bézier curve, $x^i_e(t)$ is a third-degree polynomial, and thus we can compute an exact root using the closed form expression developed by Cardano [7] during the XVI century. It can be seen that this root exists and is unique if the points are sorted in ascending order with respect to the energy axis, as is the case. A more comprehensive description of the use of Bézier curves to model the PEC can be found in [16].

It is worth noting that, since the Bézier curve representation of the PEC implicitly defines the power as a function of the energy, it is difficult to implement the whole model through a modeling language (such as AMPL or GAMS). These systems do not support implicit functions, and it is not straightforward to use external routines (e.g., to implement Cardano's equation) with their programming languages.

2.6. Generation and power constraints using the PEC

Coordination problems need a tool to deal with the relationship existing between the generation and power involved in the supply of the energy

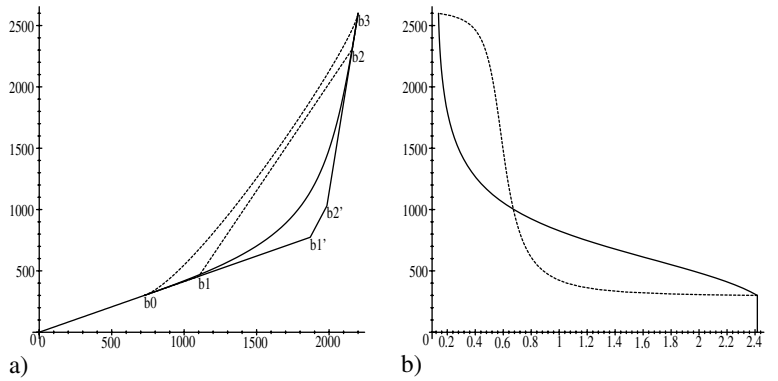

Fig. 7. Different SGDC depending on the position of the Bézier points. (a) PECs and polygonals joining Bézier points: b0-b1′-b2′-b3 (continuous), and b0-b1-b2-b3 (dashed). (b) Corresponding SGDC.

demand. Otherwise, the coverage of the SGDC becomes a very complex task unless extreme simplifications are introduced in the model. The mathematical formulation of these constraints is easily obtained using the PEC idea—and its Bézier curve based representation.

The power P_j^i supplied by the jth unit at interval i, generated by some amount of energy E_j^i, can be computed as

$$P_j^i = PE^i\left(E_j^i + \sum_{m=1}^{j-1} E_m^i + G_{\Delta m}^i\right) - PE^i\left(\sum_{m=1}^{j-1} E_m^i + G_{\Delta m}^i\right) \quad j = 1,\ldots,\mathrm{Nu},\ \ i = 1,\ldots,\mathrm{Ni}. \tag{14}$$

Bounds to the capacity can be stated for each unit using (14):

$$P_j^i \leqslant \overline{P}_j^i, \quad j = 1,\ldots,\mathrm{Nu},\ \ i = 1,\ldots,\mathrm{Ni}. \tag{15}$$

Finally, the coverage of the SGDC can be expressed as

$$PE^i\left(\sum_{j=1}^{\mathrm{Nu}} (E_j^i + G_{\Delta j}^i)\right) = \sum_{j=1}^{\mathrm{Nu}} P_j^i + \widetilde{P}_\Delta^i, \quad i = 1,\ldots,\mathrm{Ni}. \tag{16}$$

2.7. Formulation of the optimization problem

The final formulation of the hydrothermal coordination problem can be written as:

$$\begin{aligned} \text{Min}\quad & \sum_{i=1}^{\mathrm{Ni}}\left(\sum_{j=1}^{\mathrm{Nu}}\sum_{f=1}^{\mathrm{Nf}} y_{f,j}^i Z_{f,j}^i + y_X^i E_X^i\right) \\ \text{s.t.}\quad & \text{Balance hydraulic constraints} : (1),(2),(3), \\ & \text{Hydraulic generation constraints} : (4), \\ & \text{Balance thermal constraints} : (5),(6), \\ & \text{Stochastic hydrogeneration constraints} : (7),(8),(10), \\ & \text{PEC constraints} : (14),(15),(16). \end{aligned} \tag{17}$$

The objective function (17) is the minimization of the overall cost and it is made of two parts: the purchases of fuels and the use of emergency energy. The symbols $y_{f,j}^i$ and y_X^i refer to unitary costs for fuels and emergency energy respectively. The rest of the constraints have been introduced in the previous subsections.

2.8. Extensions

Several extensions have been added to the original model. Here we will only mention the most relevant. All of them have been considered and/or implemented in the HTCOOR package.

2.8.1. Contracts

The coverage of the SGDC by the thermal system can be done by means of the thermal units and through external contracts with other utilities. These contracts have been modeled as a special type of thermal unit, with the following properties:

- All contracts share a special type of (unlimited) fuel.

- Unlike thermal units, which are usually available from the first to the last interval of the period under study, each contract j has an initial R_j and final S_j interval of application. Contract generation can be restricted to these intervals by adding the following constraints:

$$E^i_{f,j} = 0, \quad i < R_j \vee i > S_j.$$

- The cost of contract j is given by the concave function:

Cost contract

$$j = \alpha_j \left(\sum_{i=R_j}^{S_j} E^i_{f,j} \right) + \beta_j \left(\sum_{i=R_j}^{S_j} E^i_{f,j} \right)^2.$$

This cost must be included in the objective function (17).

2.8.2. Pumping arcs

The inclusion of pumping arcs in the hydraulic network enables water to be transferred from down to upstream reservoirs. This is performed in low-load demand periods, as an attempt to increase the water resources at upstream reservoirs for later high-load periods. This kind of arc can be considered as a special type of discharge arc with the following properties:

- Pumping arcs mean energy consumption, whereas discharge arcs generate energy.
- The energy consumed is a function that depends on the volume of water pumped, and the initial and final volumes of the down and upstream reservoirs (for discharge arcs only the initial and final volumes of the upstream reservoir are considered).

For any arc a that pumps water from reservoir n (downstream) to reservoir n' (upstream), its energy consumption for the ith interval (PM^i_a) is computed as

$$PM^i_a = B^i_a \sum_{l=0}^{4} \gamma_l \Delta h^l,$$

where B^i_a is the amount of water pumped by this arc during the interval, γ_l are constants, and Δh represents the height the water is raised.

In the current version of HTCOOR, the pumping is simply subtracted from the hydrogeneration. This is a simple but effective strategy. A more accurate and complicated option—not yet implemented—would be to consider some of the Bézier points of the PEC as a function of the pumping.

2.8.3. Auction system

A preliminary model for the auction market system has recently been proposed. Unfortunately, the very first results obtained with the auction-extended model showed that it complicates the solution of the problem by the optimizer. The usefulness of the model is thus directly related with the availability of a robust solver.

The method suggested for modeling the auction system considers that only a subset $\mathscr{C}$ of the Nu units belong to the utility that is solving the problem. The rest of the units are those of the competitors. Information about the LDC is now associated with the total demand of the country, not only of the utility. The hydrothermal model would now provide the coverage of the SGDC for the whole country considering all the utilities involved. A particular utility can solve the problem by imposing that the generation of their units (both thermal and hydraulic) must be higher than a certain percentage of the total generation, for all the intervals. These percentages can be different for each interval, and must be appropriately forecasted by the company. The new Ni constraints to be added to the original formulation are:

$$\sum_{i=1}^{l} \sum_{\mu \in \mathscr{C}} \left(E^i + (G^i)^0 + G^i_\Delta \right)_\mu \geqslant \%_l \sum_{i=1}^{\mathrm{Ni}} \widehat{E}^i$$
$$l = 1, \ldots, \mathrm{Ni}, \tag{18}$$

where $\mathscr{C}$ denotes the set of units owned by the utility, $\sum_{\mu \in \mathscr{C}} \left(E^i + (G^i)^0 + G^i_\Delta \right)_\mu$ the total generation of the company for a particular interval, $\%_l$ the percentage parameters for each interval, and $\widehat{E}^i$ the energy demand at interval i.

The main drawback of this approach is the choice of the percentage parameters. These values must be accurately adjusted by the operator, assuming that a bad choice can easily result in an

infeasible problem. This is specially relevant when, as in the current version of the package, the optimizers used do not always guarantee a feasible solution. In these situations it is difficult to ascertain whether the infeasibilities are due to the limitations of the optimizer or to the values of the percentage parameters.

Up to now, only the thermal generation term has been considered in the constraints (18); in this case these constraints are merely linear. Including the hydrogeneration is part of the further work to be done.

3. Description of the HTCOOR package

The HTCOOR package implements the model formulated in Section 2. It is mainly written in Fortran (75% of the source, aside from the optimizer code). Only the main program and several routines are coded in C, to allow the dynamic allocation of the main vectors needed during the optimization stage. The length of the program is roughly 10,000 lines. HTCOOR can be downloaded for academic purposes from `http://www-eio.upc.es/~jcastro/htcoor.html`. A comprehensive description of the package can be found in [6].

The structure of the application is depicted in Fig. 8. The current version of the package has not been completely integrated with any data warehouse or data base, so the input/output data are still read/written from/to files. From the figure we see that the problem description is performed through five input files:

- File · `thun`: describes the thermal system.
- File · `net`: describes the hydraulic system.
- File · `load`: contains the information about the load demand.
- File · `dat`: provides general information (e.g., number of intervals, length of each interval, number of hydraulic blocks, etc.).
- Files · `inf`: contains historical data about inflows at the reservoirs of the hydraulic system.

Firstly, from the `.thun` and `.net` files, the application generates three more intermediate files:

- File · `trm`: for the thermal system.
- File · `hydro`: for the hydraulic system.
- File · `cmb`: for the fuel information (prices, availability, etc.).

Thereafter, from the three intermediate files, and the original `.load`, `.dat` and `.inf` ones, the package creates the structure of the optimization model to be solved. This procedure is dependent on the type of solver to be applied. Up to now only Minos 5.5 [19] and Snopt 5.3 [11] have been used, which basically share the same model description structure. Finally, the problem is optimized and the solution obtained—if the solver finishes successfully—is written to the file `.lis`. A detailed description of the many fields for each input file can be found in [6].

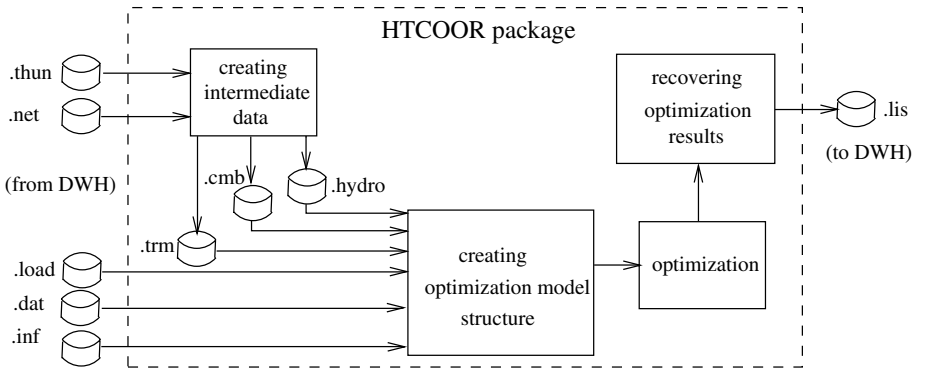

Fig. 8. Structure of the HTCOOR package.

Due to the large possible number of nonlinear variables and constraints, we considered a sparse Jacobian structure when communicating the model to the solvers. In fact, the sparsity of the model is significant for most instances. For instance, Fig. 9 represents the particular Jacobian structure for problem WW of Table 1 in Section 4. This Jacobian has 3194 variables, 380 nonlinear and 1283 linear constraints, and 21,001 nonzero elements. Note that the Jacobian is made of nested primal and dual block structures. Although these substructures are difficult to be exploited by the algorithms implemented in Minos and Snopt, they could be taken into account when using alternative solvers based in, e.g., interior-point methods [13].

It is noteworthy that the HTCOOR package does not make use of any modeling language (as, e.g., AMPL [10]). Although the use of such tools would simplify the implementation task extremely, we got some limitations. First, we needed to perform several optimizations to obtain some intermediate data for the final optimization stage. The adhoc implementation developed permitted an efficient communication among these different optimization problems. The second reason is related to the execution time: adhoc models implemented in C and Fortran are much more efficient than those obtained with modeling languages—though the latter can be coded in a fraction of the time required by the former. This second point is specially relevant since, due to the size and nonlinearities of the instances, execution times tend to be large. The last reason is that up to now modeling languages are not able to deal with constraints given by parametric curves, as those that define the power as a function of the energy through a Bézier curve representation of the PEC. The best solution would be to use an external function, which is still not a straightforward task with current modeling systems. Another alternative would be to replace the equation $p = x_p(x_e^{-1}(e))$ (power p as a function of the energy e) by the two equations $p = x_p(t)$, $e = x_e(t)$. However, this would mean adding an extra nonlinear constraint and variable—the parameter t—for each interval and thermal unit, which would approximately double the number of nonlinear constraints of the problem.

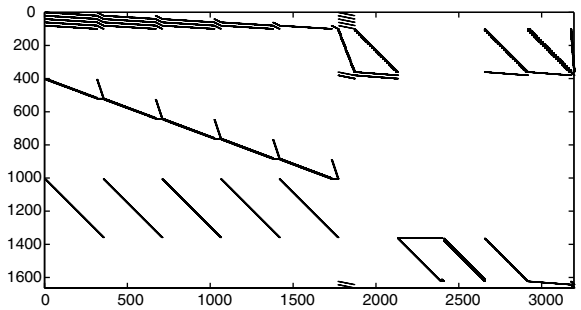

Fig. 9. Jacobian structure for problem WW of Table 1.

4. Computational results

The current release of the code HTCOOR was evaluated through a set of pseudo-real test cases. All of them were obtained by defining different configurations for the thermal and hydraulic subsystems of a base test case. This base case is a slight modification of a real one from the Spanish hydrother-

Table 1
Characteristics of the test cases

Problem	Int.	Therm.	Resvrs.	Disch.	Comm.	Vars.	Linc.	Nonlinc.	Nnz.
pp	3	13	2	3	3	250	86	51	1707
mm	6	13	3	6	5	685	246	114	4530
nn	6	13	3	6	5	685	246	114	4530
zz	8	13	1	2	5	687	200	152	4738
WW	20	13	6	12	5	3194	1283	380	21,001
DD	40	13	6	12	5	6414	2563	760	42,281
BB	15	13	41	85	5	10,314	5173	285	62,286
MM	12	70	41	85	5	11,634	4819	912	171,162
AA	33	70	41	85	5	32,340	13,303	2508	473,982

mal system, provided by a power utility. The remaining instances are a subset of this real problem.

Table 1 gives the characteristics for each instance. We grouped them into two subsets: small problems (first four rows) and large ones (last five rows). Problem AA corresponds to the real base case, and, due to its size, is a good representative of the type of problem to be solved with HTCOOR. The meaning of the columns of the table is:

- Problem: name of the problem.
- Int.: number of intervals of the planning horizon.
- Therm.: number of thermal units.
- Resvrs.: number of reservoirs.
- Disch.: total number of discharge arcs considered in the hydraulic subsystem.
- Comm.: number of commodities used to model stochasticity in the hydraulic subsystem.
- Vars.: number of variables of the optimization problem.
- Linc.: number of linear constraints of the optimization problem.
- Nonlinc.: number of nonlinear constraints of the optimization problem.
- Nnz.: number of nonzero elements (linear and nonlinear) of the Jacobian constraints matrix.

The instances were solved with Minos 5.5 [19] and Snopt 5.3 [11]. Both codes only provide solutions that are locally optimal. Therefore, and due to the nonconvexity of the problem, global solutions are not guaranteed. Tables 2 and 3 show the results obtained with each solver. The *penalty parameter* was set to 50 for Minos 5.5, to deal with the nonlinearities of the functions [19]. The parameter *scale option* was set to 1 in all the Snopt 5.3 runs [11], otherwise even for the simplest problems the algorithm stopped at a nonoptimal and nonfeasible point with a "the current point cannot be improved" message. The default values were used for the remaining parameters (for both Minos 5.5 and Snopt 5.3), except for some few executions which are clearly marked in the tables.

For each problem the following information is provided:

- Status: exit status provided by the solver. This column can take the values "optimal" (optimal solution point has been obtained), "infeasible" (problem reported as infeasible by the solver) or "too many iter." (too many iterations).
- Iter: overall number of minor iterations performed by the solver in the solutions of the subproblems. For Minos 5.5 they correspond to the minimization of a nonlinear—augmented Lagrangian—function subject to linear constraints, whereas for Snopt 5.3 they are related to quadratic programming subproblems.
- f^*: value of the objective function at the optimal solution obtained (in the same currency as the input data).
- CPU (s): CPU seconds required to perform the run. All runs were carried out on a Sun/Ultra2 2200 workstation with 200 MHz clock, 256 MB of main memory, ≈68 Mflops Linpack, 14.7 Specfp95 and 7.8 Specint95.
- CPU/iter (ms): CPU time per iteration in milliseconds.

Table 2
Results obtained with Minos 5.5

Problem	Status	Iter	f^*	CPU (s)	CPU/iter (ms)
pp	Optimal	543	8.704343672e + 9	0.41	0.76
mm	Optimal	1101	1.8336647408e + 10	2.57	2.33
nn	Optimal	775	1.8462822133e + 10	1.32	1.70
zz	Optimal	916	2.4208240477e + 10	1.49	1.63
WW	Optimal	6769	2.9152512944e + 10	81.52	12.04
DD	Optimal	10,896	2.7910024022e + 10	302.50	27.76
BB	Optimal	72,640	2.0327043893e + 10	4521.08	62.24
MM	Infeasible	281,830	–	7756.70	27.52
AA	Optimal	831,183	1.13014855496e + 11	108,916.51	131.04

Table 3
Results obtained with Snopt 5.3

Problem	Status	Iter	f^*	CPU (s)	CPU/iter (ms)
pp	Optimal	700	8.704343596e + 9	0.90	1.29
mm	Optimal	2615	1.8349202899e + 10	8.02	3.07
nn	Optimal	2833	1.8471176724e + 10	8.58	3.03
zz	Optimal	1352	2.4203322733e + 10	2.67	1.98
WW*	Optimal	32,552	2.9154089151e + 10	947.21	29.10
DD	Optimal	79,596	2.7965381364e + 10	15,600.22	195.99
BB	Optimal	192,137	2.0348450144e + 10	195,936.96	1019.78
MM	Optimal	81,060	1.96798275462e + 11	301,440.21	3718.73
MM**	Optimal	74,744	1.96827415432e + 11	160,868.84	2152.26
AA***	Too many iter.	1,500,000	1.14929788079e + 11	704,391.3	469.59

* Real workspace was increased.
** Problem solved with *scale option parameter* different than 1.
*** The code got stuck; it stopped in a feasible but nonoptimal point.

It should be noted that the parameters had to be specifically tuned for some problems. In general we can say that no combination of values—of those tested—for the Minos and Snopt parameters guaranteed the solution of all the problems. This made the solution of the different instances a nontrivial task, usually performed following a trial-and-error parameter adjusting. Moreover, the efficiency of the code was quite different depending on the values of the parameters (see, e.g., rows MM and MM** in Table 3). Minos solved all the problems but case MM, which was reported as infeasible. However, this problem is in fact feasible, as shown by the Snopt run. Snopt also failed in the solution of only one problem, instance AA, where it seemed to get stuck, moving from one major iteration to another without performing any minor iteration. For problem AA, Snopt stopped at a feasible but nonoptimal point. For problem WW, following a suggestion of one of the authors of Snopt (P.E. Gill), we considerably increased the real workspace used by the solver. Otherwise, Snopt got stuck with a final "too many major iterations" message.

Table 4 shows the ratios of the number of iterations, CPU time, and CPU time per iteration between Snopt and Minos, only for those problems successfully solved by both solvers; two rows show the average values for the small and large instances. It is clear than Minos was considerably more efficient than Snopt at solving the model implemented in HTCOOR. As for the number of iterations, Snopt performed, in average, 2.2 and 4.9 times more than Minos for, respectively, the small and large problems. The CPU time per iteration was also favorable to Minos, with average ratios of 1.5 for the small and 8.6 for the large instances. This made Minos, in average, 3.4 and 35.5 times faster than Snopt for each subset of problems. Clearly, the efficiency of Minos is better for the large problems.

It is not a straightforward task to give a precise explanation of the better performance of Minos without knowing the details of the implementation of both codes. In principle, differences can not be explained because Minos and Snopt reached far apart local optimum points. Looking at the f^* columns of Tables 2 and 3, we see that, despite the

Table 4
Iteration, CPU, and CPU per iteration ratios between Snopt 5.3 and Minos 5.5

Problem	Iter. ratio	CPU ratio	CPU/iter. ratio
pp	1.3	2.2	1.7
mm	2.4	3.1	1.3
nn	3.7	6.5	1.8
zz	1.5	1.8	1.2
Average	2.2	3.4	1.5
WW	4.8	11.6	2.4
DD	7.3	51.6	7.1
BB	2.7	43.3	16.4
Average	4.9	35.5	8.6

nonconvexity of the problem, both packages returned similar objective function values. Moreover, we observed that these objective values correspond to similar optimal points. One possible argument for the different performance would be that, due to the highly nonlinear constrains of the model, the augmented Lagrangian objective function considered by Minos [21] (which includes the constraints) behaves better than the quadratic approximation of a modified Lagrangian used by Snopt [12] (that only includes a quadratic—and possibly poor—approximation of the constraints). Although that forces Minos to perform more objective and constraints function evaluations than Snopt (e.g., in problem DD, Minos and Snopt required 9656 and 293 function evaluations, respectively), it could explain why it requires far less iterations. The worser CPU time per iteration of Snopt can be due to a larger number of superbasic variables. The number of superbasic variables is the dimension of the linear systems of equations to be solved at each minor iteration of the codes—which are related with a quasi-Newton approximation of a projected Hessian [20]. For instance, in problem DD, Minos and Snopt finished with 38 and 527 superbasic variables, respectively. A similar behaviour was observed for the other instances.

5. Conclusions

From the computational results reported it can be stated that the model implemented in the HTCOOR package for hydrothermal coordination seems to be a difficult one for nonlinear solvers based on projected augmented Lagrangian (Minos) and sequential quadratic programming (Snopt) algorithms. Moreover, it requires the tuning of some of the default settings of these codes to work properly. The model can thus be useful for evaluating alternative optimization algorithms (e.g., interior-point methods for nonlinear nonconvex problems that only require first derivatives). Having a more reliable code would make it possible to solve larger and more difficult hydrothermal instances, even extending the model for the auction market system. In fact, one of the reasons that prevented this latter extension was the unavailability of a robust and efficient solver for this model. Adding this and additional features to HTCOOR is part of the further work to be done.

Acknowledgements

The authors are indebted to N. Nabona for his helpful comments and suggestions about the model. The authors also thank M. Saunders and P.E. Gill for their help with Minos and Snopt.

References

[1] T.W. Archibald, C.S. Buchanan, L.C. Thomas, K.I.M. McKinnon, Controlling multi-reservoir systems, European Journal of Operational Research 129 (3) (2001) 619–626.
[2] H. Balériaux, E. Jamoulle, F. Linard, Simulation de l'explotation d'un parc de machines thermiques de production d'électricité couplé à des stations de pompage, Revue Électricité de la Societé Royale Belge des Électriciens 5 (7) (1967) 225–245.
[3] P. Bézier, Procédé de définition numérique des courbes et surfaces non mathématiques, Automatisme 12 (5) (1968) 189–196.
[4] W. Böhm, G. Farin, J. Kahmann, A survey of curve and surface methods in CAGD, Computer Aided Geometric Design 1 (1984) 1–60.
[5] J. Castro, N. Nabona, An implementation of linear and nonlinear multicommodity network flows, European Journal of Operational Research 92 (1996) 37–53.
[6] J. Castro, J.A. González, HTCOOR program documentation, Technical Report DR2000-12, Statistics and Operations Research Department, Universitat Politècnica de Catalunya, 2000. Available from <http://www-eio.upc.es/~jcastro>.
[7] L. Childs, A Concrete Introduction to Linear Algebra, UTM Springer-Verlag, New York, 1979.
[8] L.F. Escudero, C. García, J.L. de la Fuente, F.J. Prieto, Hydropower generation management under uncertainty via scenario analysis and parallel computation, IEEE Transactions of Power Systems 11 (2) (1996) 683–689.
[9] L.F. Escudero, J.L. de la Fuente, C. García, F.J. Prieto, A parallel computation approach for solving multistage stochastic network problems, Annals of Operations Research 90 (1999) 131–160.
[10] R. Fourer, D.M. Gay, B.W. Kernighan, AMPL: A Modeling Language for Mathematical Programming, Duxbury Press, 1993.
[11] P.E. Gill, M.A. Saunders, W. Murray, User's Guide for SNOPT 5.3: A Fortran Package for Large-Scale Nonlinear Programming, Report NA 97-5, Department of Mathematics, University of California, 1998.

[12] P.E. Gill, M.A. Saunders, W. Murray, SNOPT: An SQP algorithm for large-scale constrained optimization, SIAM Journal on Optimization 12 (2002) 979–1006.

[13] J. Gondzio, R. Sarkissian, Parallel interior-point solver for structured linear programs, Technical Report MS-00-025, Department of Mathematics and Statistics, The University of Edinburgh, 2000.

[14] J.A. González, Stochastic issues on long-term hydrothermal coordination (in Spanish), Ph.D. thesis, Statistics and Operations Research Department, Universitat Politècnica de Catalunya, 1997. Available from <ftp://ftp-eio.upc.es/pub/onl/tesis/tesi-jaga.ps.gz>.

[15] J.A. González, Probabilistic production costing modeled with AMPL, IEEE Transactions on Power Systems 17 (2002) 277–282.

[16] J.A. González, J. Castro, The long-term hydrothermal coordination model implemented in the HTCOOR package, Technical Report DR2000-11, Statistics and Operations Research Dept., Universitat Politècnica de Catalunya, 2000. Available from <http://www-eio.upc.es/~jcastro>.

[17] Y. Ikura, G. Gross, G.S. Hall, PG&E's state-of-the-art scheduling tool for hydro systems, Interfaces 16 (1986) 65–82.

[18] A.B. Kumar, S. Vemuri, P. Ebrahimzadeh, N. Farahbakhshian, Fuel resource scheduling—the long-term problem, IEEE Transactions on Power Systems 1 (1986) 145–151.

[19] B.A. Murtagh, M.A. Saunders, MINOS 5.0. User's guide, Department of Operations Research, Stanford University, USA, 1983.

[20] B.A. Murtagh, M.A. Saunders, Large-scale linearly constrained optimization, Mathematical Programming 14 (1978) 41–72.

[21] B.A. Murtagh, M.A. Saunders, A projected Lagrangian algorithm and its implementation for sparse nonlinear constraints, Mathematical Programming Study 16 (1982) 84–117.

[22] N. Nabona, Multicommodity network flow model for long-term hydrogeneration optimization, IEEE Transactions on Power Systems 8 (2) (1993) 395–404.

[23] N. Nabona, J. Castro, J.A. González, Optimum long-term hydrothermal coordination with fuel limits, IEEE Transactions on Power Systems 10 (2) (1995) 1054–1062.

[24] M.V.F. Pereira, L.M.V.G. Pinto, Multi-stage stochastic optimization applied to energy planning, Mathematical Programming 52 (1991) 359–375.

[25] V.R. Sherkat, R. Campo, K. Moslehi, E.O. Lo, Stochastic long-term hydrothermal optimization for a multireservoir system, IEEE Transactions on Power Apparatus and Systems 104 (1985) 2040–2050.

[26] A.J. Wood, B.F. Wollenberg, Power Generation Operation and Control, Wiley, New York, 1984.